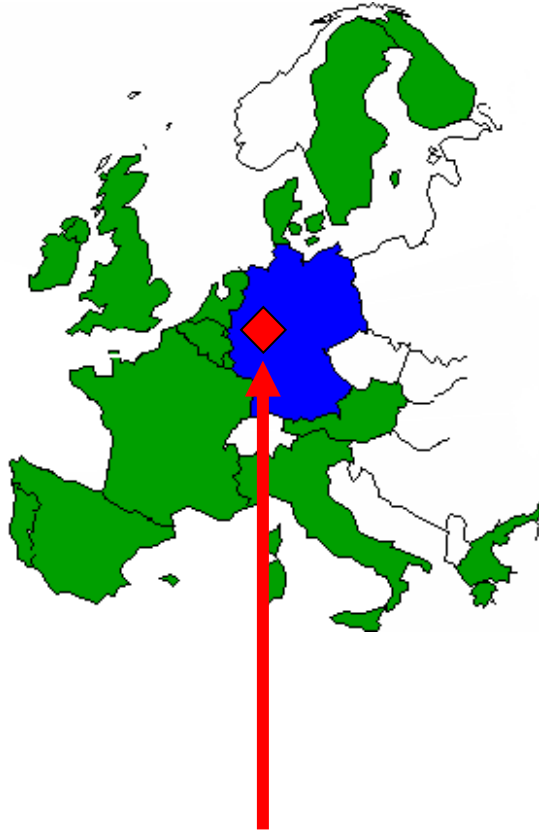


**And now
for something
completely different...**



**(Picture courtesy
of Python M)**



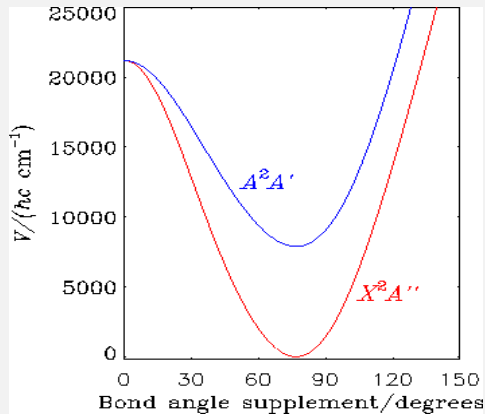
*Where is
Wuppertal?*



The Wuppertal monorail



The general scheme of things (at least in this lecture....)

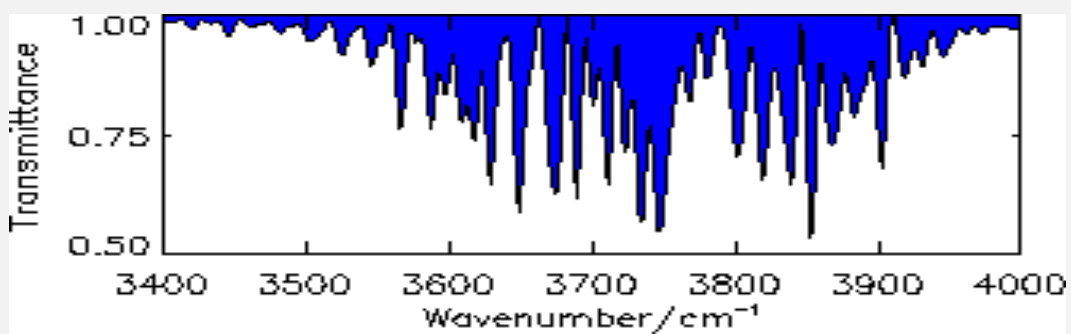


Potential energy surface(s)
Dipole moment surface(s) ...

in general obtained from *ab initio* calculations

PROGRAMS MORBID,
RENNER, DR, TROVE

Simulated rotation-vibration spectra



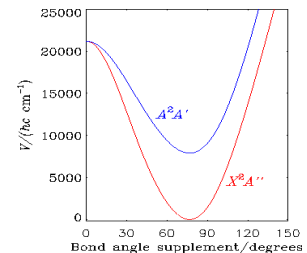
Nuclear-motion programs developed:

MORBID (Morse Oscillator Rigid Bender Internal Dynamics, 1988)

triatomic molecule in isolated electronic state

RENNER (Renner Effect, 1995)

triatomic molecule in Renner-degenerate states



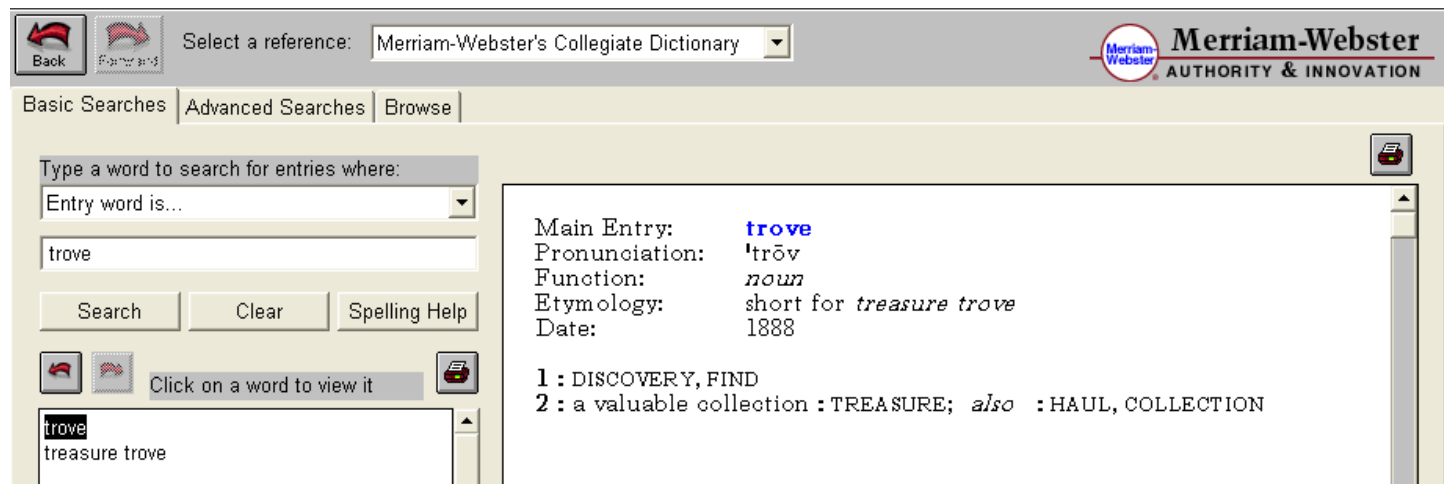
DR (Double Renner, 2004)

triatomic molecule in double-Renner-degenerate states

TROVE (Theoretical ROtation-Vibration Energies, 2007)

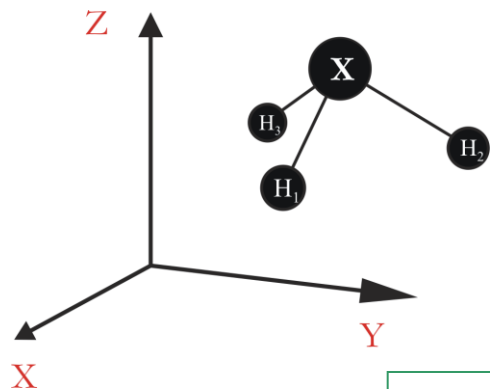
(*in principle*) any molecule in isolated electronic state

TROVE: Theoretical ROVibrational Energies: Variational calculations of rotation-vibration for a general polyatomic molecule in an isolated electronic state



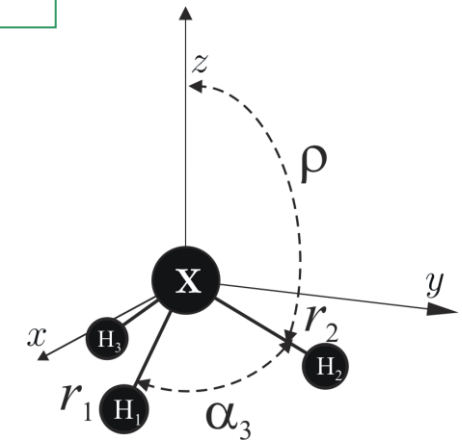
Hamiltonian: Coordinate transformation

$$\left(\sum_{i=1}^N \frac{-\hbar^2}{2M_i} \nabla_i^2 + V \right) \Psi = E\Psi$$



Laboratory fixed
Cartesian
coordinate system

Body fixed internal
coordinate system



$$\mathbf{R}_i = \mathbf{R}^{\text{CM}} + S^{-1}(\theta, \phi, \chi) [\mathbf{R}_i^{\text{MS}}(\mathbf{r})]$$

$$\left[\frac{1}{2} \sum_{\lambda=1}^{3N} \sum_{\mu=1}^{3N} \Pi_{\lambda} G_{\lambda,\mu}(\mathbf{r}) \Pi_{\mu} + U(\mathbf{r}) + V(\mathbf{r}) \right] \Psi = E\Psi$$

Different molecules – different transformations?

If we now let ω be a four-dimensional column vector containing the three angular velocities ω_x , ω_y , ω_z , and $\omega_p = \dot{\rho}$ (see Section (2.3) of Ref. (J)), the classical kinetic energy is given by Eq. (17) of HBJ, which we quote

$$T = \frac{1}{2} \omega^T \mathbf{I} \omega + \sum_{\alpha=x,y,z} \omega_\alpha \mathbf{S}^T \mathbf{A}^T \mathbf{M} \mathbf{M}^\alpha \mathbf{A} \mathbf{S} + \omega_p \left[\frac{d\mathbf{A}}{d\rho} \right]^T \mathbf{M} \mathbf{A} \mathbf{S} + \frac{1}{2} \mathbf{S}^T \mathbf{G}^{-1} \mathbf{S}. \quad (14)$$

The 4×4 I matrix is given by Eq. (20) of HBJ; the G matrix is given by Eq. (3.22) of Ref. (6); M is a 9×9 diagonal matrix with $M_{11} = M_{22} = M_{33} = m_1$, $M_{44} = M_{55} = M_{66} = m_2$, and $M_{77} = M_{88} = M_{99} = m_3$; and \mathbf{M}^α ($\alpha = x, y, z$) is a 9×9 Meal and Polo matrix that forms vector cross products (24). Superscript T denotes transposition of the matrix.

The first step in transforming Eq. (14) into a quantum mechanical kinetic energy operator is to express it in terms of the coordinates and their conjugate momenta $J_\alpha = \partial T / \partial \omega_\alpha$, and $P_i^{(S)} = \partial T / \partial S_i$. This is done by following the procedure described in Chapter 11 of Ref. (25), and the result is

$$T = \frac{1}{2} \sum_{\alpha,\beta=x,y,z,p} (J_\alpha - p_\alpha) \mu_{\alpha\beta} (J_\beta - p_\beta) + \frac{1}{2} \sum_{i,j=1,3} P_i^{(S)} G_{ij} P_j^{(S)} \quad (15)$$

with the following definitions: The 4×4 μ matrix is the inverse of the symmetrical matrix I' whose elements are given by

$$\begin{aligned} I'_{\alpha\alpha} &= \sum_{i=1}^3 m_i (a_{i\beta}^2 + a_{i\delta}^2) + 2 \sum_{i=1}^3 \sum_{l=1,3} m_i (a_{il} A_{i\beta,l} + a_{il} A_{i\delta,l}) S_l \\ &\quad + \sum_{i=1}^3 \sum_{l,u=1,3} m_i (A_{il,l} A_{il,u} + A_{il,l} A_{il,u}) S_l S_u - \mathbf{S}^T \mathbf{A}^T \mathbf{M} \mathbf{M}^\alpha \mathbf{A} (\mathbf{A}^T \mathbf{M} \mathbf{M}^\alpha \mathbf{A})^T \mathbf{S}, \quad (16) \\ I'_{\alpha\beta} &= - \sum_{i=1}^3 m_i (a_{i\alpha} a_{i\beta}) - \sum_{i=1}^3 \sum_{l=1,3} m_i (a_{il} A_{i\beta,l} + a_{il} A_{i\delta,l}) S_l \\ &\quad - \sum_{i=1}^3 \sum_{l,u=1,3} m_i (A_{il,l} A_{il,u} + A_{il,l} A_{il,u}) S_l S_u - \mathbf{S}^T \mathbf{A}^T \mathbf{M} \mathbf{M}^\alpha \mathbf{A} (\mathbf{A}^T \mathbf{M} \mathbf{M}^\alpha \mathbf{A})^T \mathbf{S}, \quad (17) \end{aligned}$$

where (α, β, δ) is a cyclic permutation of (x, y, z) . Further,

$$I'_{\alpha\beta} = -2 \left[\frac{da}{d\rho} \right]^T \mathbf{M} \mathbf{M}^\alpha \mathbf{A} \mathbf{S} + \mathbf{S}^T \mathbf{A}^T \mathbf{M} \mathbf{M}^\alpha \frac{d\mathbf{A}}{d\rho} \mathbf{S} - \mathbf{S}^T \mathbf{A}^T \mathbf{M} \mathbf{M}^\alpha \mathbf{A} G \left(\left[\frac{d\mathbf{A}}{d\rho} \right]^T \mathbf{M} \mathbf{A} \right)^T \mathbf{S}, \quad (18)$$

$$\begin{aligned} I'_{\alpha\beta} &= \left[\frac{da}{d\rho} \right]^T \mathbf{M} \frac{da}{d\rho} - 2 \left[\frac{d^2 a}{d\rho^2} \right]^T \mathbf{M} \mathbf{A} \mathbf{S} + \mathbf{S}^T \left[\frac{da}{d\rho} \right]^T \mathbf{M} \frac{da}{d\rho} \mathbf{S} \\ &\quad - \mathbf{S}^T \left[\frac{da}{d\rho} \right]^T \mathbf{M} \mathbf{A} \mathbf{G} \left(\left[\frac{da}{d\rho} \right]^T \mathbf{M} \mathbf{A} \right)^T \mathbf{S}, \quad (19) \end{aligned}$$

for $\alpha = x, y, z$. The quantity a is a nine-dimensional column vector analogous to d , bolding the nine components of the $a_i(\rho)$ vectors. Finally, the vibrational angular momenta p_α are given by

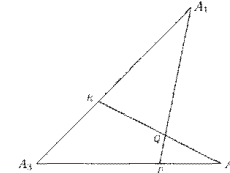


Fig. 1. Internal coordinate system of Sutcliffe and Tennyson [15]: A_i represents atom i . The coordinates are given by $r_1 = A_2 - R$, $r_2 = A_1 - R$ and $\theta = A_1 Q A_2$. The geometric parameters are defined by $g_1 = (A_3 - P)/(A_3 - A_2)$ and $g_2 = (A_3 - R)/(A_3 - A_1)$.

where V is the electronic potential. Symmetrised angular basis functions for \hat{H} can be written [11]

$$|j, k, p\rangle = 2^{-1/2} (1 + \delta_{k0})^{-1/2} [\Theta_{jk}(\theta) |JMk\rangle + (-1)^p \Theta_{j-k}(\theta) |JM-k\rangle], \quad (2)$$

where $|JMk\rangle$ is a rotation matrix element [27] and Θ_{jk} an associated Legendre polynomial [28]. The total parity is given by $(-1)^{j+p}$ with $p = 0$ or 1 for e or f states, respectively. k is the projection of the total angular momentum, J , along the body-fixed z axis which can be chosen parallel to either r_1 or r_2 .

Letting \hat{H} act on $|j, k, p\rangle$, multiplying from the left by $\langle j', k', p'|$ and integrating over all angular coordinates yields an effective, diagonal in p , Hamiltonian [11]

$$\hat{K}_{jj'}^{(1)} = \delta_{jj'} \delta_{kk'} \left[\frac{\hbar^2}{2\mu_1} \frac{\partial^2}{\partial r_1^2} - \frac{\hbar^2}{2\mu_2} \frac{\partial^2}{\partial r_2^2} + \frac{1}{2} \hbar^2 (j+1) \left(\frac{1}{\mu_1 r_1^2} + \frac{1}{\mu_2 r_2^2} \right) \right], \quad (3)$$

$$\begin{aligned} \hat{K}_{jj'}^{(2)} &= -\delta_{jj'+1} \delta_{kk'} d_{jk} \frac{\hbar^2}{2\mu_{12}} \left(\frac{\partial}{\partial r_1} - \frac{j+1}{r_1} \right) \left(\frac{\partial}{\partial r_2} - \frac{j+1}{r_2} \right) \\ &\quad - \delta_{jj'-1} \delta_{kk'} d_{jk-1,k} \frac{\hbar^2}{2\mu_{12}} \left(\frac{\partial}{\partial r_1} + \frac{j}{r_1} \right) \left(\frac{\partial}{\partial r_2} + \frac{j}{r_2} \right), \end{aligned} \quad (4)$$

$$\hat{K}_{jj'}^{(3)} = \delta_{jj'} \delta_{kk'} \frac{\hbar^2}{2\mu_1 r_1^2} (J(J+1) - 2k^2) - \delta_{jj'} \delta_{kk'+1} \frac{\hbar^2}{2\mu_1 r_1^2} (1 + \delta_{k0} + \delta_{k'0})^{1/2} C_{jk}^\pm C_{jk}^\pm, \quad (5)$$

$$\begin{aligned} \hat{K}_{jj'}^{(4)} &= \delta_{jj'+1} \delta_{kk'+1} \frac{\hbar^2}{2\mu_{12}} (1 + \delta_{k0} + \delta_{k'0})^{1/2} C_{jk}^\pm \frac{a_{j\pm k}}{r_1} \left(\frac{j+1}{r_2} - \frac{\partial}{\partial r_2} \right) \\ &\quad + \delta_{jj'-1} \delta_{kk'+1} \frac{\hbar^2}{2\mu_{12}} (1 + \delta_{k0} + \delta_{k'0})^{1/2} C_{jk}^\pm \frac{b_{j+k}}{r_1} \left(\frac{j}{r_2} + \frac{\partial}{\partial r_1} \right), \end{aligned} \quad (6)$$

The angular factors in the above equations are

$$C_{jk}^\pm = [J(J+1) - k(k \pm 1)]^{1/2}, \quad (7)$$

$$d_{jk} = \left[\frac{(j-k+1)(j+k+1)}{(2j+1)(2j+3)} \right]^{1/2}, \quad (8)$$

Different molecules – different transformations?

subsequently deriving the kinetic energy operator caused substantial algebraic problems. One significant outcome of this research is that we now believe that if we were to repeat all our work on the derivation of kinetic energy operators for three- and four-atom molecules using the necessary distinct coordinate systems, we would use the Podolsky formalism described in section 3.1. This needs only the evaluation of the Wilson \mathbf{G} matrix and the Jacobian J . Thus we believe that our advocacy of the chain rule approach [10] is not optimum for these problems.

S.C. would like to acknowledge financial support from the Leverhulme Trust and from the US Office of Naval Research, in particular the encouragement of Dr. Peter Schmidt is much appreciated. N.C.H. would like to acknowledge support from Professor K. Hirao for a visit to Tokyo, where this research commenced.

Appendix A

The kinetic energy operator for ammonia

The vibration–vibration terms are the Wilson σ^{μ} [21]. The contribution to the Hamiltonian is twice this $I \neq J$, and every term is multiplied by $-\frac{1}{2}$.

$$\frac{1}{\mu} = \frac{1}{m_1} + \frac{1}{m_2}. \quad (\text{A } 1)$$

$$s1 = \sin\left(\frac{\theta_1}{2}\right), \quad s2 = \sin\left(\frac{\theta_2}{2}\right), \quad s3 = \sin\left(\frac{\theta_3}{2}\right),$$

$$c1 = \cos\left(\frac{\theta_1}{2}\right), \quad c2 = \cos\left(\frac{\theta_2}{2}\right), \quad c3 = \cos\left(\frac{\theta_3}{2}\right).$$

$$\frac{\partial^2}{\partial \theta_1^2} \sigma^{11} = \frac{1}{\mu},$$

$$\frac{\partial^2}{\partial \theta_2 \partial \theta_1} \sigma^{12} = \frac{1}{m_2} [1 - 2 \sin^2 \theta_2],$$

$$\frac{\partial^2}{\partial \theta_3 \partial \theta_1} \sigma^{13} = \frac{1}{m_3},$$

$$\frac{\partial^2}{\partial \theta_1 \partial \theta_2} \sigma^{21} = \frac{1}{m_1} [1 - 2 \sin^2 \theta_1],$$

$$\frac{\partial^2}{\partial \theta_3 \partial \theta_2} \sigma^{23} = \frac{1}{m_3} [1 - 2 \sin^2 \theta_3],$$

$$\frac{\partial^2}{\partial \theta_1 \partial \theta_3} \sigma^{31} = \frac{1}{m_1},$$

$$\frac{\partial^2}{\partial \theta_2 \partial \theta_1} \sigma^{41} = \frac{2\beta}{m_2} \left[\frac{3\cos^2 \beta - (-2\sqrt{1 - \beta^2})\beta + 3}{r_2} \right],$$

$$\frac{\partial^2}{\partial \theta_3 \partial \theta_1} \sigma^{43} = \frac{2\beta}{m_3} \left[\frac{1 + 2\beta^2 + (\beta^2 - 1)}{r_3} \right],$$

$$\begin{aligned} \frac{\partial^2}{\partial \theta_1^2} \sigma^{44} &= \frac{\cos^2 \beta r_0^2}{\mu^2 r_1^2 r_2^2} + \frac{\cos^2 \beta + 1^2}{\mu^2 r_1^2 r_3^2} + \frac{\cos^2 \beta + \epsilon^2}{\mu^2 r_2^2 r_3^2} \\ &- 2 \cot^2 \beta \ln \frac{1 + 2\beta^2 + \sin^2 \beta}{[r_1 r_2 r_3]^2} \\ &- 2 \cot^2 \beta \frac{1 + 2\beta^2 + \sin^2 \beta}{[r_1 r_2 r_3]^2} \\ &+ \frac{2(-2 \cot^2 \beta + \beta) \ln [1 + 2\beta^2] + 2\beta^2 \cos^2 \beta / \ln [1 - \beta]}{[r_1 r_2 r_3]^2}, \\ \frac{\partial^2}{\partial \theta_2 \partial \theta_1} \sigma^{51} &= \frac{2\beta}{m_2} \left[\frac{2 + \cos^2 \beta}{r_2} + \frac{(-3\beta) \sin^2 \beta + 2\beta}{r_1} \right], \\ \frac{\partial^2}{\partial \theta_3 \partial \theta_2} \sigma^{52} &= \frac{2\beta}{m_3} \left[\frac{1 + \cos^2 \beta}{r_3} + \frac{(3\beta) \sin^2 \beta - 1}{r_2} \right], \\ \frac{\partial^2}{\partial \theta_2 \partial \theta_3} \sigma^{53} &= \frac{2 \sin^2 \beta}{m_2} \left[\frac{1 + 1}{r_2} + \frac{1 + 2\beta^2}{r_3} \right], \\ \frac{\partial^2}{\partial \theta_2 \partial \theta_2} \sigma^{54} &= \frac{-2\beta \cos^2 \beta}{\mu^2 r_1^2 r_3^2} + \frac{-3\beta \cos^2 \beta}{\mu^2 r_1^2 r_2^2} + \frac{-1 \cos^2 \beta - 2\beta^3}{\mu^2 r_2^2 r_3^2} \\ &+ \frac{[2 \cot^2 \beta + \epsilon^2] (2 \cos^2 \beta - 2 \cot^2 \beta - 1) + 2\beta^2 \sin^2 \beta}{[r_1 r_2 r_3]^2}, \\ &+ \frac{[-2 + 2 \cot^2 \beta + \epsilon^2] (2 \cos^2 \beta - 1 + 2\beta^2 \sin^2 \beta) - 4(2\beta^2 \cos^2 \beta)}{[r_1 r_2 r_3]^2}, \\ &+ \frac{[-2\epsilon^2 \cos^2 \beta + \epsilon^2] (2 \cos^2 \beta - 1 - 2\beta^2 \sin^2 \beta) - 4(3\beta^2 \cos^2 \beta)}{[r_1 r_2 r_3]^2}, \\ \frac{\partial^2}{\partial \theta_3^2} \sigma^{55} &= \frac{\cos^2 \beta + \epsilon^2}{\mu^2 r_2^2} + \frac{\cos^2 \beta + \epsilon^2}{\mu^2 r_1^2} + \frac{\cos^2 \beta + \epsilon^2}{\mu^2 r_3^2} \\ &- 2 \cot^2 \beta \frac{1 + 2\beta^2 + \sin^2 \beta}{[r_1 r_2 r_3]^2} \\ &- 2 \cot^2 \beta \frac{1 + 2\beta^2 + \sin^2 \beta}{[r_1 r_2 r_3]^2} \\ &+ \frac{2(-3 \cos^2 \beta + \epsilon^2) (2 + 1 + 2\beta^2) + 2\beta^2 \cos^2 \beta / \ln [1 - \beta]}{[r_1 r_2 r_3]^2}, \\ \frac{\partial^2}{\partial \theta_2 \partial \theta_1} \sigma^{61} &= -\frac{\cos \beta \sin \beta}{m_2} \left[\frac{2\beta^2 + 2\beta^2}{r_2} \right], \\ \frac{\partial^2}{\partial \theta_3 \partial \theta_2} \sigma^{62} &= -\frac{\cos \beta \sin \beta}{m_3} \left[\frac{1 + 1}{r_3} + \frac{1 + 2\beta^2}{r_1} \right], \\ \frac{\partial^2}{\partial \theta_2 \partial \theta_3} \sigma^{63} &= \frac{-\cos \beta \sin \beta}{m_2} \left[\frac{1 + 1}{r_2} + \frac{1 + 2\beta^2}{r_1} \right], \\ \frac{\partial^2}{\partial \theta_2 \partial \theta_2} \sigma^{64} &= \frac{-2\beta \cos \beta}{2m_2 r_1^2 r_3^2} + \frac{1 + 2\beta \cos \beta}{2m_2 r_1^2 r_2^2} + \frac{1 + 3 \cos \beta}{2m_2 r_2^2 r_3^2} \\ &+ \frac{[\cot \beta (1 + 2\beta^2 + 2\beta^2) + 2\beta^2 \cos \beta] \sin \beta (r_1^2 + r_2^2)}{[2m_2 r_1 r_2 r_3]^2}, \\ &+ \frac{[\cot \beta (-2 + 2\beta^2 + 2\beta^2) + 2\beta^2 \cos \beta] \sin \beta (-r_1^2 + 1 + 2\beta^2)}{[2m_2 r_1 r_2 r_3]^2}, \\ &+ \frac{[\cot \beta (-2 + 3\beta^2 + 1 + 2\beta^2) + 2\beta^2 \cos \beta] \sin \beta (-2 + 3 + 1 + 2\beta^2)}{[2m_2 r_1 r_2 r_3]^2}, \\ \frac{\partial^2}{\partial \theta_3 \partial \theta_2} \sigma^{65} &= \frac{-3\beta \cos \beta}{2m_3 r_1^2 r_2^2} + \frac{4\beta \cos \beta}{2m_3 r_1^2 r_3^2} + \frac{-1 + 2\cos \beta}{2m_3 r_2^2 r_3^2} \\ &+ \frac{[\cot \beta (1 + 2\beta^2 + 2\beta^2) + 2\beta^2 \cos \beta] \sin \beta (r_1^2 + r_2^2)}{[2m_3 r_1 r_2 r_3]^2}, \\ &+ \frac{[\cot \beta (-2 + 1 + 2\beta^2 + 2\beta^2) + 2\beta^2 \cos \beta] \sin \beta (-r_1^2 + 1 + 2\beta^2)}{[2m_3 r_1 r_2 r_3]^2}, \\ &+ \frac{[\cot \beta (2 + 2\beta^2 + 1 + 2\beta^2) + 2\beta^2 \cos \beta] \sin \beta (-2 + 2 + 1 + 2\beta^2)}{[2m_3 r_1 r_2 r_3]^2}, \end{aligned}$$

 TABLE I. Ammonia geometry and inversion energy calculated using many basis sets and the CCSD(T) method and the B3LYP density functional.^a

Number basis	r_{eq} (Å)	θ_{eq} (Deg.)	$E_{\text{tot}}^{(\text{eq})}$ (au)	r_{st} (Å)	$E_{\text{tot}}^{(\text{st})}$ (au)	Δ_{inv} (cm ⁻¹)
B3LYP-DZVP	20	1,018,868	106,6311	-56,564,040.5	1,004,190	-56,554,867.4
B3LYP/cc-pVTZ	72	1,013,837	106,4776	-56,584,725.3	0,996,617	-56,576,286.4
B3LYP/aug-cc-pVTZ	115	1,013,049	107,2293	-56,588,857.5	0,997,438	-56,581,536.7
CCSD(T)-cc-pVDZ	29	1,027,316	103,5536	-56,402,802.2	1,005,140	-56,388,657.2
CCSD(T)-cc-pVQZ	50	1,023,670	105,9298	-56,425,519.9	1,005,433	-56,416,255
CCSD(T)-cc-pVQZ	72	1,014,098	105,6518	-56,473,197.3	0,995,127	-56,463,000.8
CCSD(T)-aug-cc-pVQZ	115	1,014,909	106,3911	-56,480,562.6	0,997,501	-56,471,739.2
CCSD(T)-aug-cc-pVQZ	145	1,012,407	106,1759	-56,493,053.0	0,994,873	-56,483,823.6
CCSD(T)-aug-cc-pVQZ	218	1,012,769	105,5304	-56,495,732.4	0,995,978	-56,487,226.1
Expt.		1,011,68	106,648			1884. ^b

^aNumber basis is the number of Gaussian basis functions in the *ab initio* calculation; r_{eq} and θ_{eq} are the bond length and valence angle for ammonia in its equilibrium pyramidal configuration; r_{st} is the bond length for ammonia in its planar configuration; $E_{\text{tot}}^{(\text{eq})}$ and $E_{\text{tot}}^{(\text{st})}$ are the total energy (electronic plus nuclear repulsion) for ammonia in the equilibrium and planar configurations, respectively; Δ_{inv} is the difference between the energy of the minimum of the PES and that of the saddle point.

^bTaken from Ref. 37.

^cTaken from Ref. 9.

where

$$\begin{aligned} f_{rs}^{(0)} &= \frac{1}{4} J^{-2} g^{(S_1 S_2)} \frac{\partial J}{\partial S_1} \frac{\partial J}{\partial S_2} - \frac{1}{2} J^{-1} \frac{\partial g^{(S_1 S_2)}}{\partial S_r} \frac{\partial J}{\partial S_s} \\ f_{rs}^{(1)} &= \frac{\partial g^{(S_1 S_2)}}{\partial S_r}, \\ f_{rs}^{(2)} &= g^{(S_1 S_2)}. \end{aligned} \quad (14)$$

The Jacobian for the two-dimensional problem is given by

$$J = 2r^6 |S_2| \frac{\sin^3 \theta}{\sqrt{1 - \cos^2 \theta + 2 \cos^3 \theta}}, \quad (15)$$

where $\theta = 2\pi/3 - S_2^2/\sqrt{3}$ and $r = R_e + S_1/\sqrt{3}$. The reciprocal metric tensor elements are

$$\begin{aligned} g^{(S_1 S_1)} &= \frac{1}{m_1} + \frac{1}{m_2} + \frac{2}{m_3} \cos \theta, \\ g^{(S_2 S_2)} &= \frac{1}{r^2 S_2^2} \left(\frac{1}{2m_1} + \frac{1 + 2 \cos \theta}{2m_2} \right. \\ &\quad \left. + \frac{1 + \cos \theta - 2 \cos^2 \theta}{2m_3} \right), \\ g^{(S_1 S_2)} &= \frac{1}{m_1 m_2 S_2^2} \frac{\cos \theta - \cos 2\theta}{\sin \theta}. \end{aligned} \quad (16)$$

The first and the second derivatives of the Jacobian with respect to S_1 and S_2 , and the first derivatives of the reciprocal metric tensor elements are given as supplementary material.³⁴

By applying l'Hospital's rule, it is seen that there are no singularities in the equations expressing the Jacobian, the \mathbf{g} -tensor matrix elements and their derivatives, even though many of these terms possess the indeterminate form 0/0. This can create some numerical instabilities that will be dealt with later.

B. Potential energy surface

Before calculating the bidimensional PES, we tested some basis sets to be used both with the CCSD(T) *ab initio* method and the B3LYP density functional approach. The results together with a comparison with experimental data³⁵ are reported in Table I. As it can be seen, there is a large improvement in the calculation of the inversion barrier when diffuse functions are added to the basis set. The basis sets, which were selected for the calculations, are the aug-cc-pVTZ, cc-pVQZ, and aug-cc-pVQZ bases of Dunning and coworkers.^{38,39} The acronyms cc-pVXZ indicate consistent polarized valence X zeta basis set, where X reads T (triple) or Q (quadruple) in our case. The prefix "aug" means augmented and refers to the presence of diffuse functions necessary to describe accurately molecular anions, Rydberg states or, as in the present case, the lone pair of electrons present in ammonia. The time required for the computation of the energy at one point of the PES is about 15 min with the aug-cc-pVTZ basis set, 1 h with cc-pVQZ, and about 8 h with the largest basis set we tried, aug-cc-pVQZ. All calculations have been performed on an SGI ORIGIN 2000 computer at the CSC computer center in Helsinki using the GAUSSIAN 98 program.⁴⁰

With the smallest basis set (aug-cc-pVTZ), we calculated a grid of 630 points (45 for the S_1 coordinate and 14 for S_2). With the cc-pVQZ basis, we calculated 208 single points (16 \times 13), whereas 162 points have been calculated for the aug-cc-pVQZ basis set (18 \times 9).

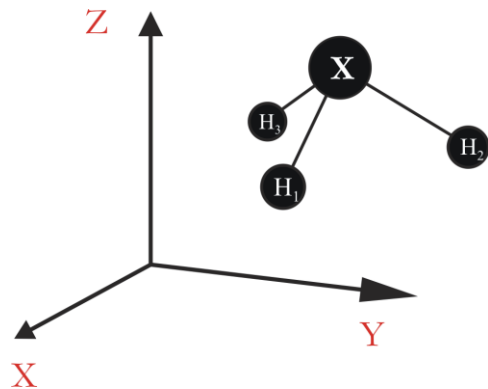
The most important regions of the PES are the two minima and the region around the saddle point, but because we have to calculate integrals involving highly excited states, it is also important to have a good description of the PES quite far from these regions. We could determine how large the grid should have been after some preliminary tests were made with the smallest basis sets. We decided to calculate a grid within the following boundaries:

$$0.6 \text{ Å} \leq r \leq 2.5 \text{ Å}, \quad (17)$$

$$70^\circ \leq \theta \leq 120^\circ. \quad (18)$$

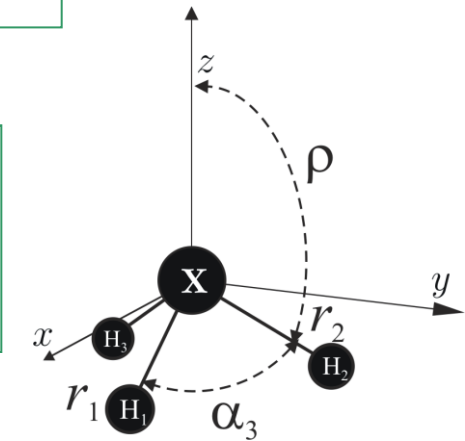
One transformation for all molecules?

$$\left(\sum_{i=1}^N \frac{-\hbar^2}{2M_i} \nabla_i^2 + V \right) \Psi = E\Psi$$



Laboratory fixed
Cartesian
coordinate system

Body fixed internal
coordinate system



- The coordinate transformation is part of the program

$$\left[\frac{1}{2} \sum_{\lambda=1}^{3N} \sum_{\mu=1}^{3N} \Pi_\lambda G_{\lambda,\mu}(\mathbf{r}) \Pi_\mu + U(\mathbf{r}) + V(\mathbf{r}) \right] \Psi = E\Psi$$

TROVE input/output: Example for PH₃

(CALCULATION OF VIBRATION ENERGIES FOR PH₃)

KinOrder 4 (Max order in the kinetic energy expansion)

PotOrder 8 (Max order in the potential energy expansion)

Natoms 4 (Number of atoms)

Nmodes 6 (Number of modes = 3*Natoms-6)

SYMGROUP C3v(M)

MOLTYPE XY3

ZMAT

P 0 0 0 0 30.9737620

H 1 0 0 0 1.00782505

H 1 2 0 0 1.00782505

H 1 2 3 0 1.00782505

END

(ACTIVE SPACE CUTOFFS:)

PRIMITIVES

Npolyads 12 (how many polyads we calculate)

enercut 80000. (energy cut in the primitive matrix for the diagonalization)

END

CONTRACTION

Npolyads 10 (how many polyads we calculate)

enercut 40000.

END

DIAGONALIZER

SYEVR

uplimit 20000.

END

Equilibrium

re 1 1.41472670

alphae 0 93.5650 deg

End

POTEN

NPARAM 304

POT_TYPE poten_xy3_morbid_10

COEFF list (powers or list)

ve 1 0.00000

fa1 0 0.00000000

fa2 1 298640.22539958

fa3 1 -657821.88828746

Gamma i value j k t quanta

A2 1 3367.019766 (A1 ; 0 0 0)(A2 ; 0 0 0 0 2 1)

A2 2 3434.732694 (A1 ; 0 0 0)(A2 ; 0 0 1 0 1 0)

A2 3 4374.979251 (A1 ; 0 0 0)(A2 ; 0 0 0 0 3 1)

A2 4 4432.311782 (A1 ; 0 0 0)(A2 ; 0 0 1 0 2 0)

A2 5 4551.397155 (A1 ; 0 0 0)(A2 ; 0 0 1 1 0 1)

E 1 1120.428678 (A1 ; 0 0 0)(E ; 0 0 0 0 1 0)

E 2 2124.197672 (A1 ; 0 0 0)(E ; 0 0 0 0 2 0)

E 3 2246.161352 (A1 ; 0 0 0)(E ; 0 0 0 1 0 1)

E 4 2332.278613 (A1 ; 0 0 0)(E ; 0 0 1 0 0 0)

E 5 3127.037913 (A1 ; 0 0 0)(E ; 0 0 0 0 3 0)

E 6 3251.100085 (A1 ; 0 0 0)(E ; 0 0 0 2 0 1)

E 7 3326.893359 (A1 ; 0 0 0)(E ; 0 0 1 1 0 0)

E 8 3354.040233 (A1 ; 0 0 0)(E ; 0 0 0 3 0 0)

E 9 3438.080699 (A1 ; 0 0 0)(E ; 0 0 1 0 1 0)

E 10 3447.234128 (A1 ; 0 0 0)(E ; 0 0 1 0 1 0)

E 11 4127.595304 (A1 ; 0 0 0)(E ; 0 0 0 0 3 1)

E 12 4254.655503 (A1 ; 0 0 0)(E ; 0 0 0 2 0 2)

E 13 4321.461208 (A1 ; 0 0 0)(E ; 0 0 1 1 1 0)

E 14 4363.730368 (A1 ; 0 0 0)(E ; 0 0 0 4 0 0)

E 15 4438.742531 (A1 ; 0 0 0)(E ; 0 0 1 0 2 0)

E 16 4454.002539 (A1 ; 0 0 0)(E ; 0 0 1 0 2 0)

E 17 4467.354459 (A1 ; 0 0 0)(E ; 0 0 0 1 0 3)

E 18 4488.128547 (A1 ; 0 0 0)(E ; 0 0 0 2 1 1)

E 19 4539.100532 (A1 ; 0 0 0)(E ; 0 0 1 2 0 0)

E 20 4556.932983 (A1 ; 0 0 0)(E ; 0 0 1 1 0 1)

E 21 4565.116007 (A1 ; 0 0 0)(E ; 0 0 1 1 0 1)

E 22 4574.932525 (A1 ; 0 0 0)(E ; 0 0 2 0 0 0)

E 23 4660.179762 (A1 ; 0 0 0)(E ; 1 0 1 0 0 0)

TROVE: Summary

Variational calculations

For a general molecule of arbitrary structure, arbitrary basis sets or coordinates

Approximate kinetic energy operator

OpenMP parallelization

FBR method (not DVR)

Accuracy & Efficiency

For one large amplitude motion

Black-box program

Intensity simulations

Vibrational contraction
of the basis set

Robust symmetrization

Basis sets:

Lanczos diagonalization
(large matrices)

Harmonic oscillator

Automatic labeling of the levels

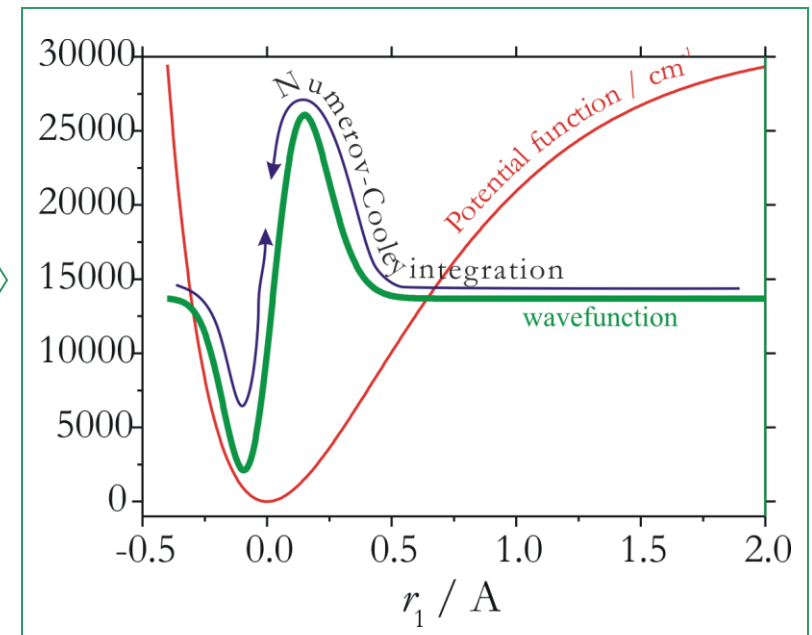
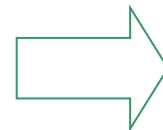
Morse oscillator

“Numerov-Cooley” solutions

1D vibrational basis functions

- ☞ Harmonic oscillator functions
- ☞ Morse oscillator functions
- ☞ Numerical function generated by Numerov-Cooley integration

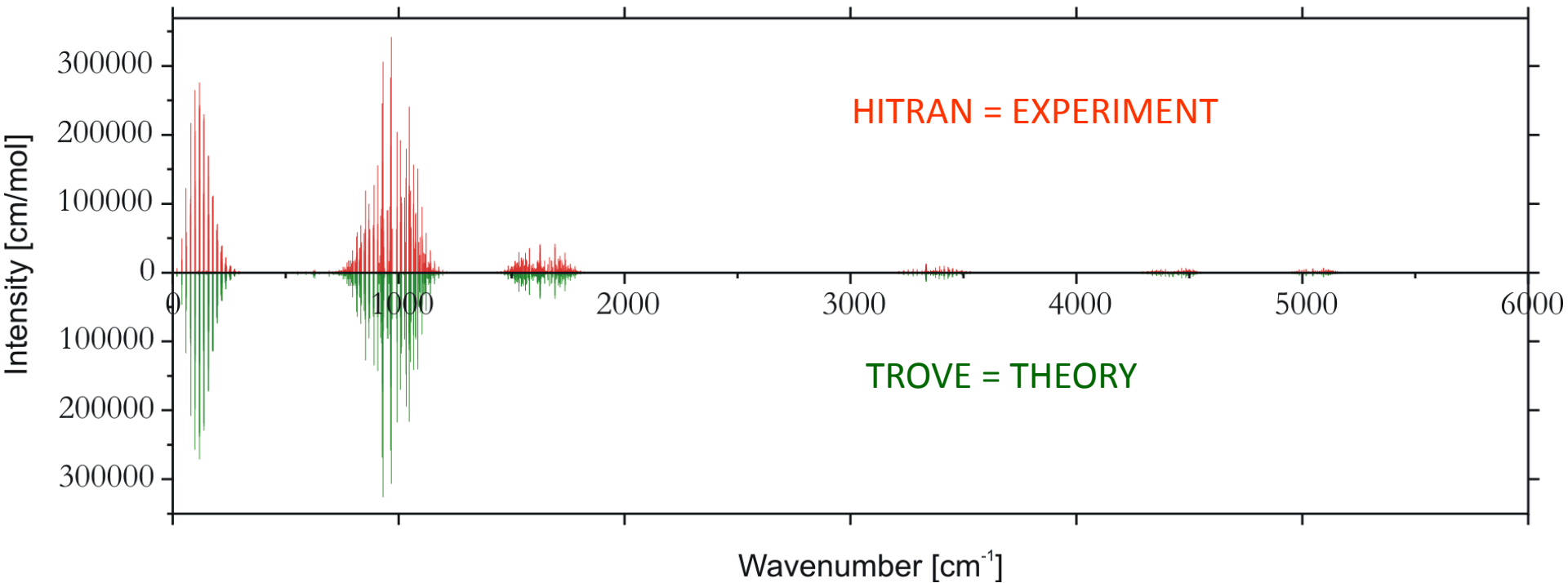
$$H_{\text{str.}}^{\text{1D}} \psi_{i_s}^{\text{1D}} = E_{i_s}^{\text{str.}} \psi_{i_s}^{\text{1D}}$$



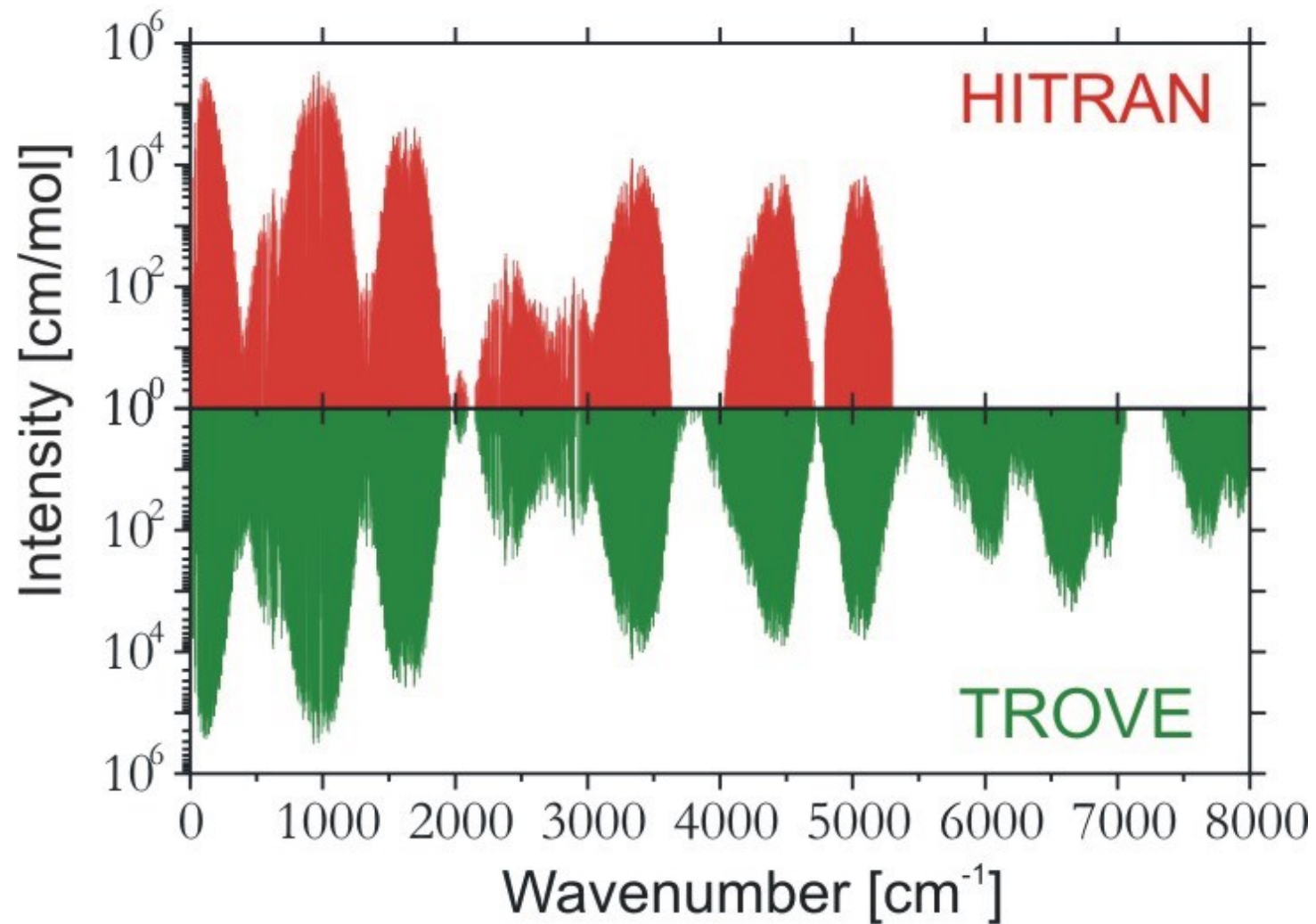
Other programs/contributors in this area (Not exhaustive . No ranking intended...)

- DEWE and GENIUSH (A. G. Császár and E. Mátyus)
- MULTIMODE (J. Bowman and S. Carter)
- T. Carrington
- H. Guo
- N. C. Handy and S. Carter
- D. Lauvergnat and A. Nauts
- D. W. Schwenke
- J. Tennyson
- ...

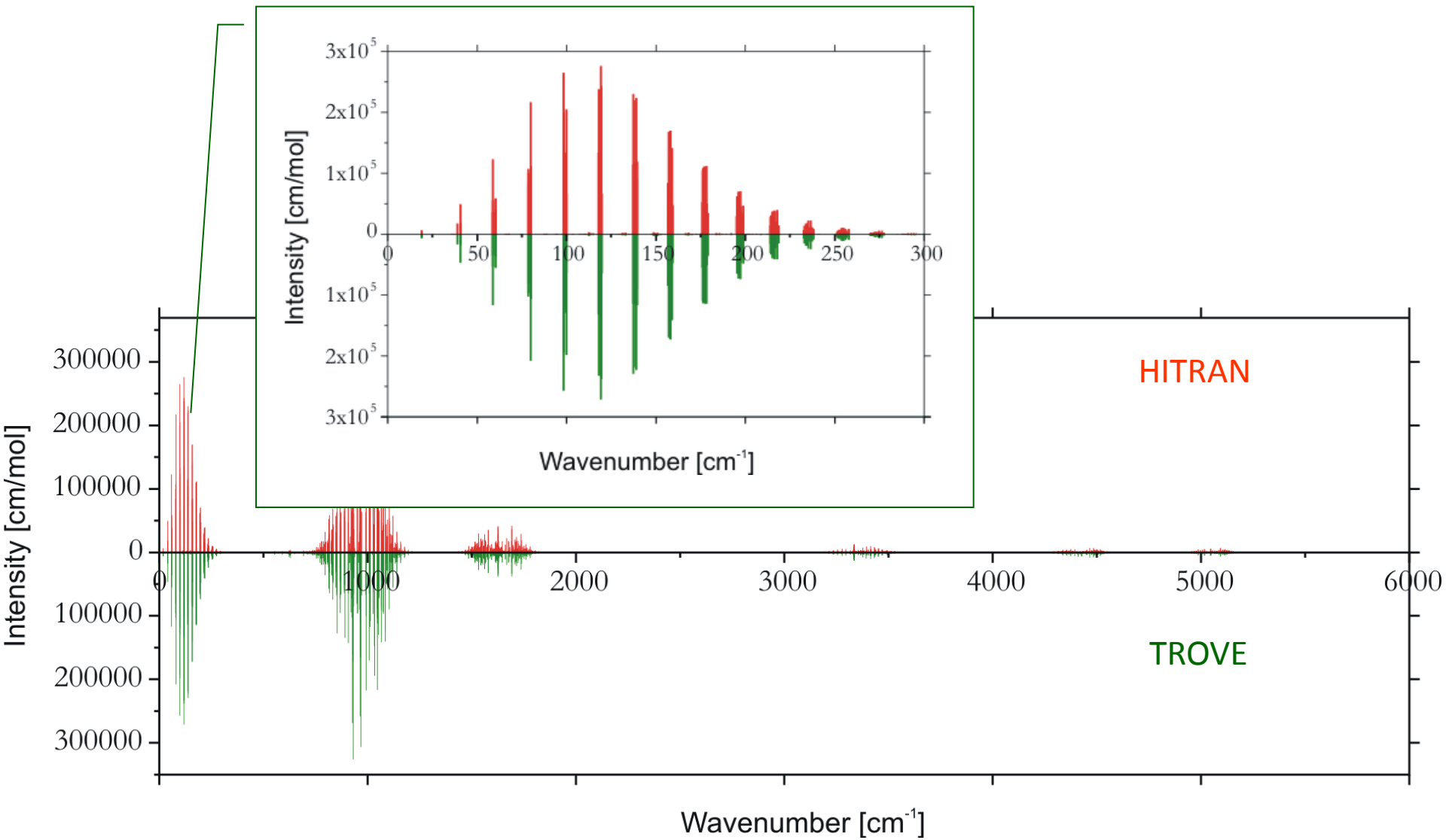
TROVE for NH₃: Absorption intensities at T=300K, 3.25 million transitions



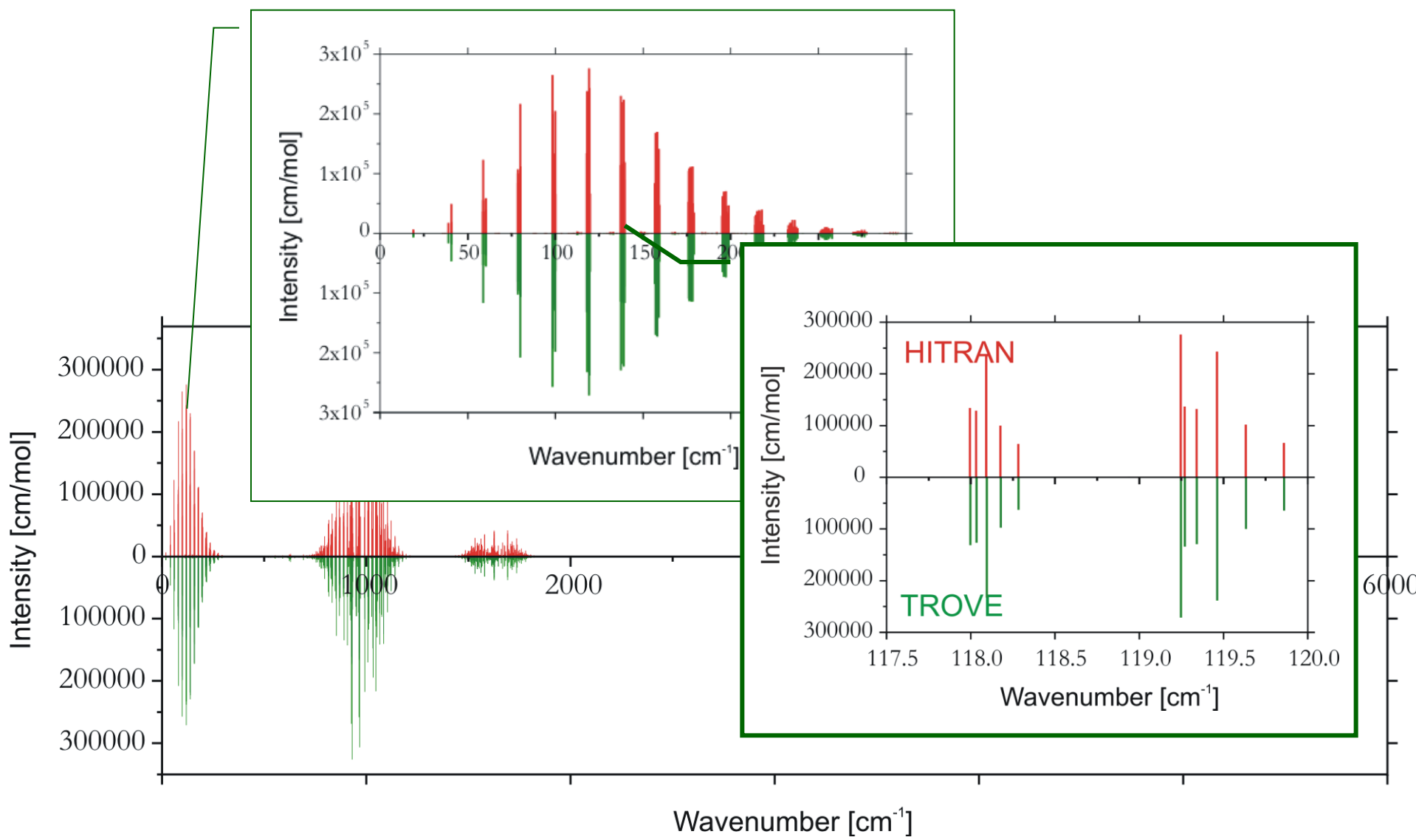
Ammonia line list simulations



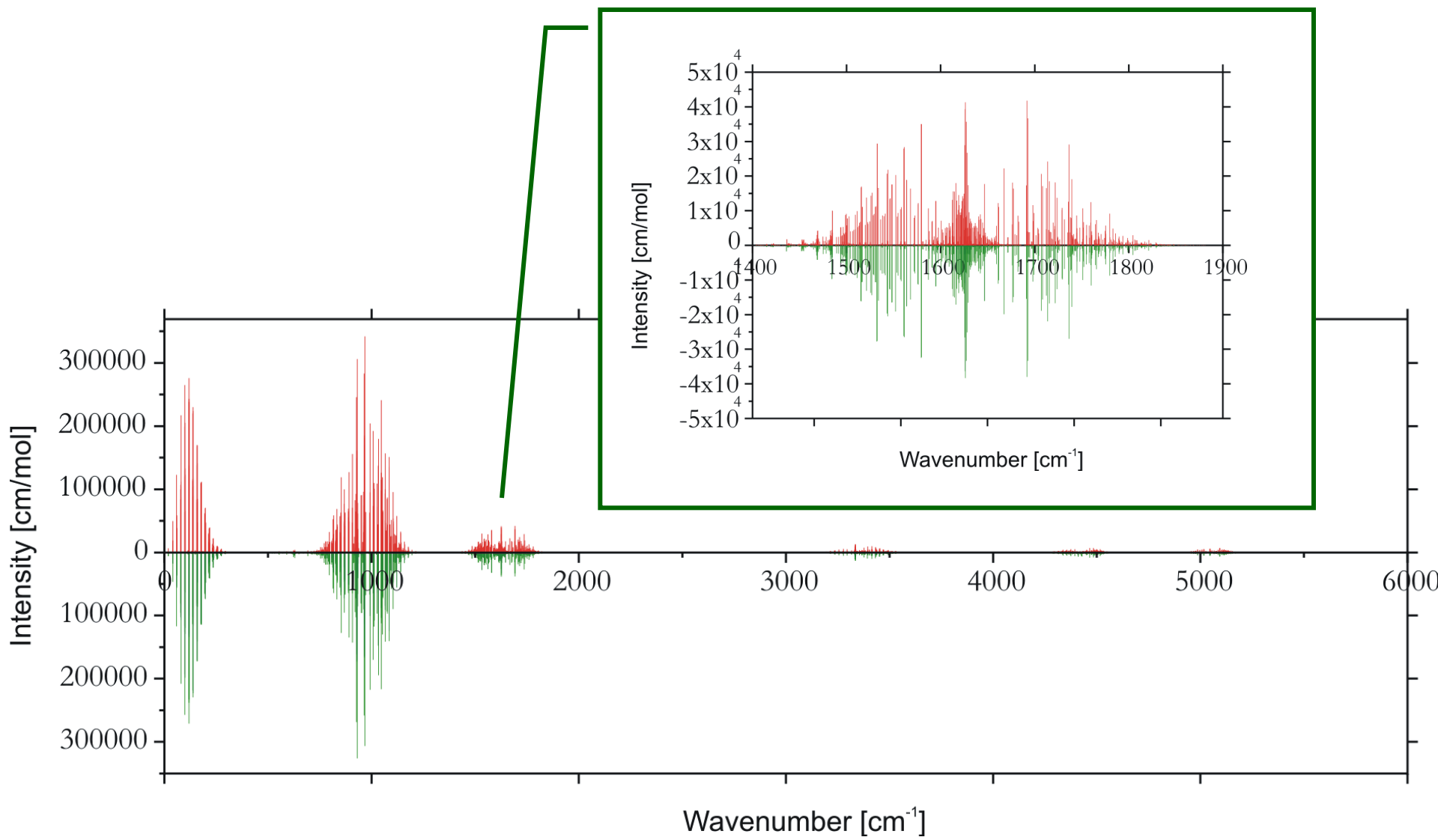
Absorption spectrum of NH₃ at T = 300 K



Absorption spectrum of NH₃ at T = 300 K

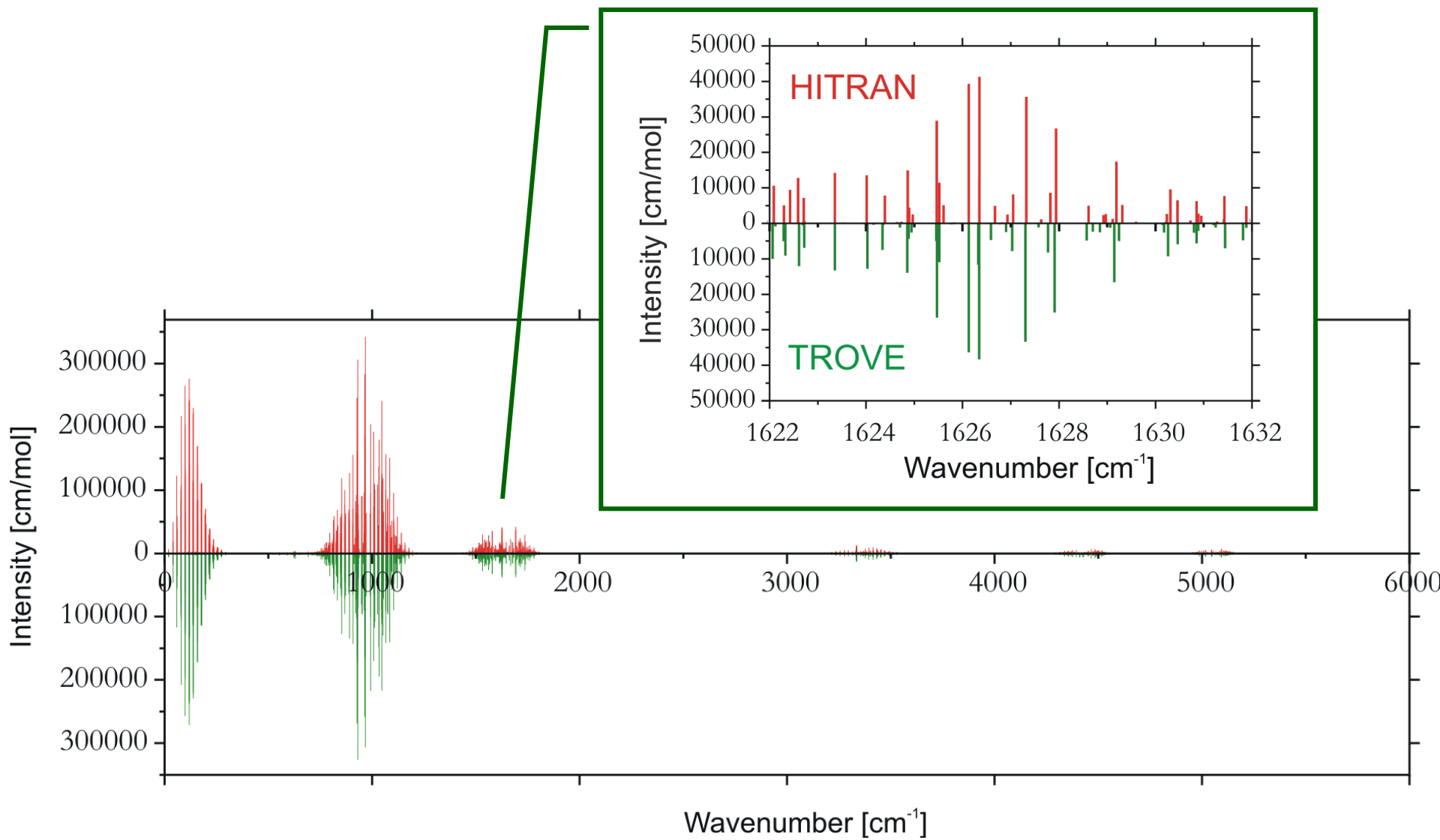


Absorption spectrum of NH₃ at T = 300 K (2v₂/v₄ bands)



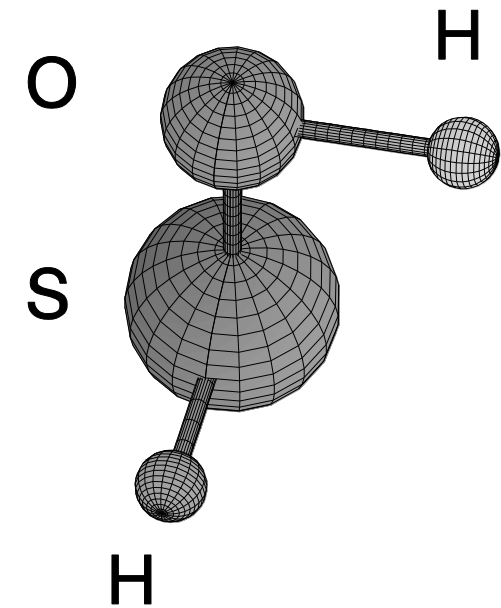
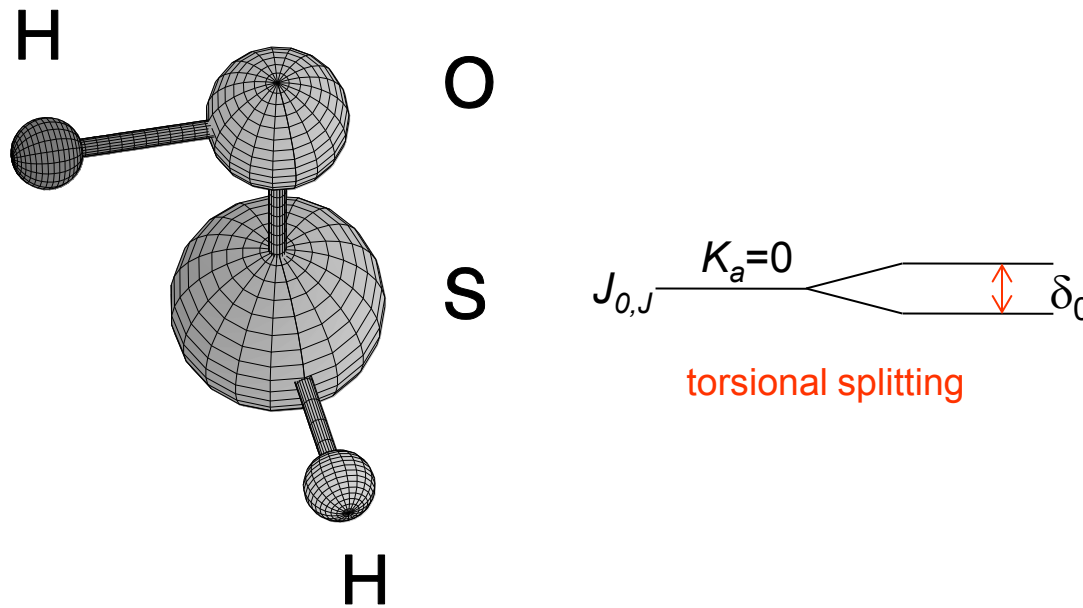
Absorption spectrum of NH₃ at T = 300 K (2v₂/v₄ bands)

Improvements under way!

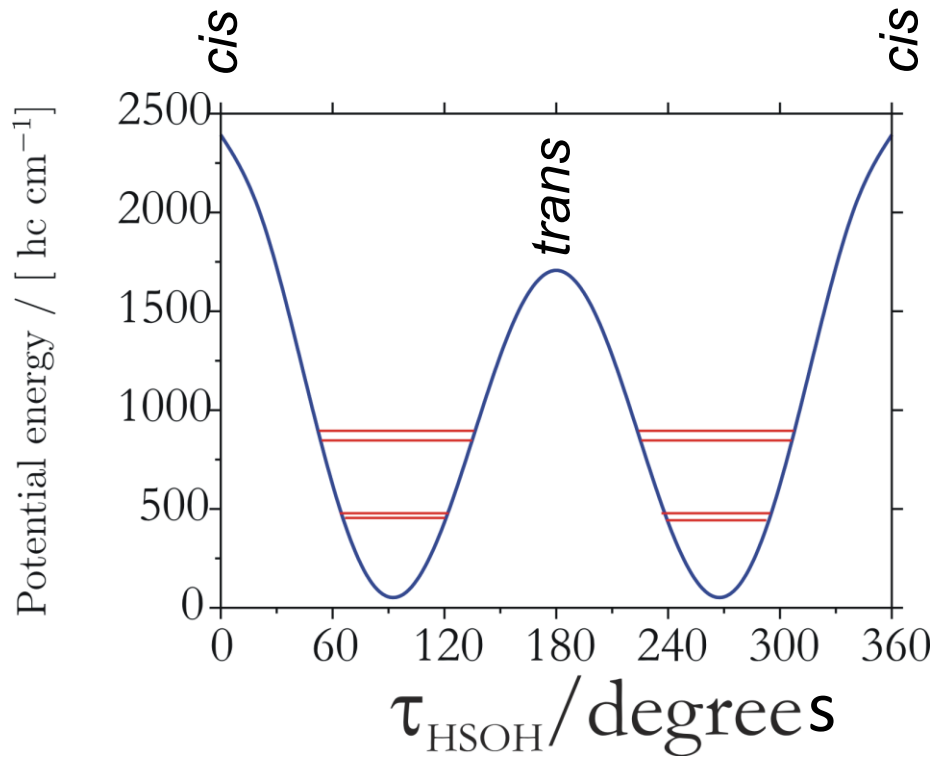
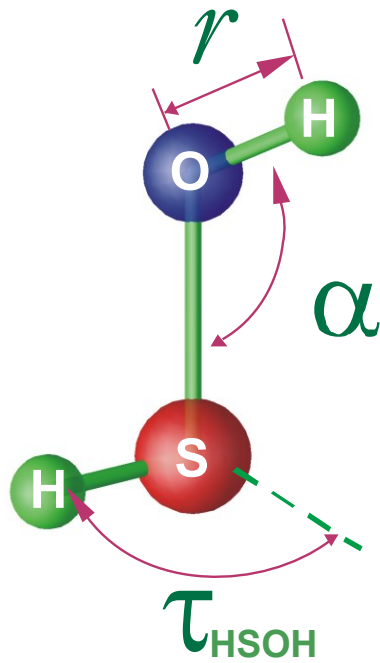


Torsional splittings and anomalous intensities in HSOH

- Two enantiomer minima
- Internal rotation about the SO bond, strongly coupled to the rotation about the a axis (associated with K_a)
- Torsional splittings



HSOH: Torsional potential



Torsional splittings show
strong variation with K_a

HOOH, HSSH, HNCNH: Splittings “stagger” with K_a

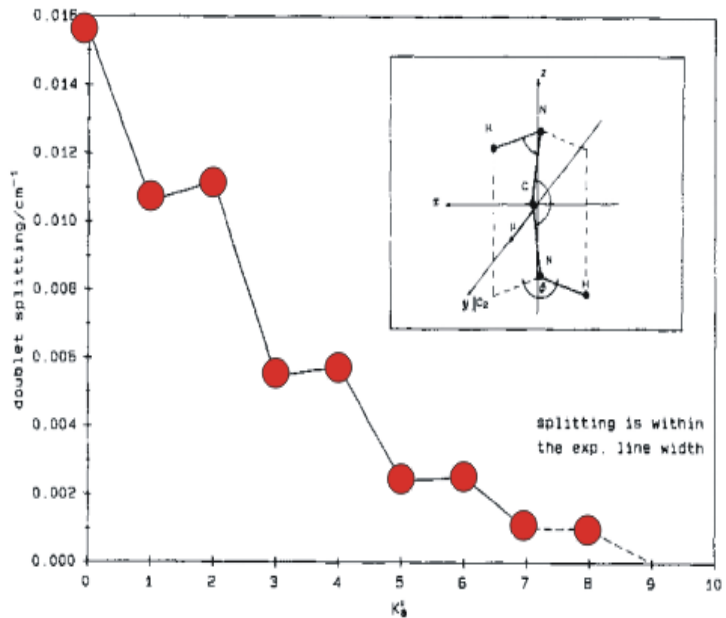


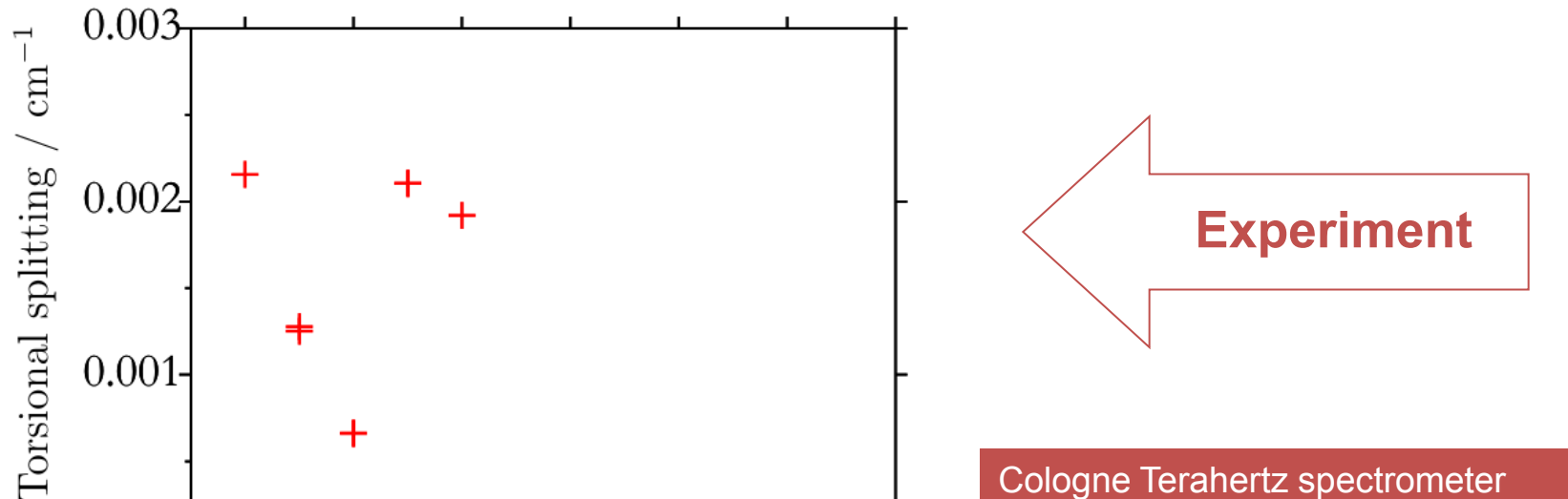
FIG. 13. Dependence of the torsional doublet splitting on K_a . The doublet splitting averaged over all J -values was obtained from the line positions of the ' Q_0 ' branch for $K_a = 0$, the ' R_{K_a} ' branch for $K_a = 1$ to $K_a = 4$, the ' R_{K_a} ' and ' Q_{K_a} ' branches for $K_a = 5$ and 6 , and from an analysis of the linewidth for $K_a = 7$. For $K_a = 8$ the splitting is identical to that for $K_a = 7$ within the experimental accuracy. For $K_a = 9$, no broadening of the ' R_{K_a} ' lines due to torsional doubling could be detected.

Example: HNCNH

Experiment: M. Birk, M. Winnewisser,
J. Mol. Spectrosc. **136**, 402 (1989)

Semi-empirical explanation by Hougen
and co-workers for HOOH and HSSH:
J.T. Hougen, *Can. J. Phys.* **62**, 1392 (1984).
J.T. Hougen, B.M. DeKoven, *J. Mol. Spectrosc.* **98**, 375 (1983).

HSOH: No staggering, more complicated variation



Experiment

Cologne Terahertz spectrometer

First observation (for $K_a \leq 3$) in 2003

M. Behnke, J. Suhr, S. Thorwirth, F. Lewen, H. Lichau, J. Hahn, J. Gauss, K.M.T. Yamada, G. Winnewisser, *J. Mol. Spectrosc.* **221**, 121 (2003)

G. Winnewisser, F. Lewen, S. Thorwirth, M. Behnke, J. Hahn, J. Gauss, and E. Herbst, *Chem. Eur. J.* **9**, 5501 (2003)

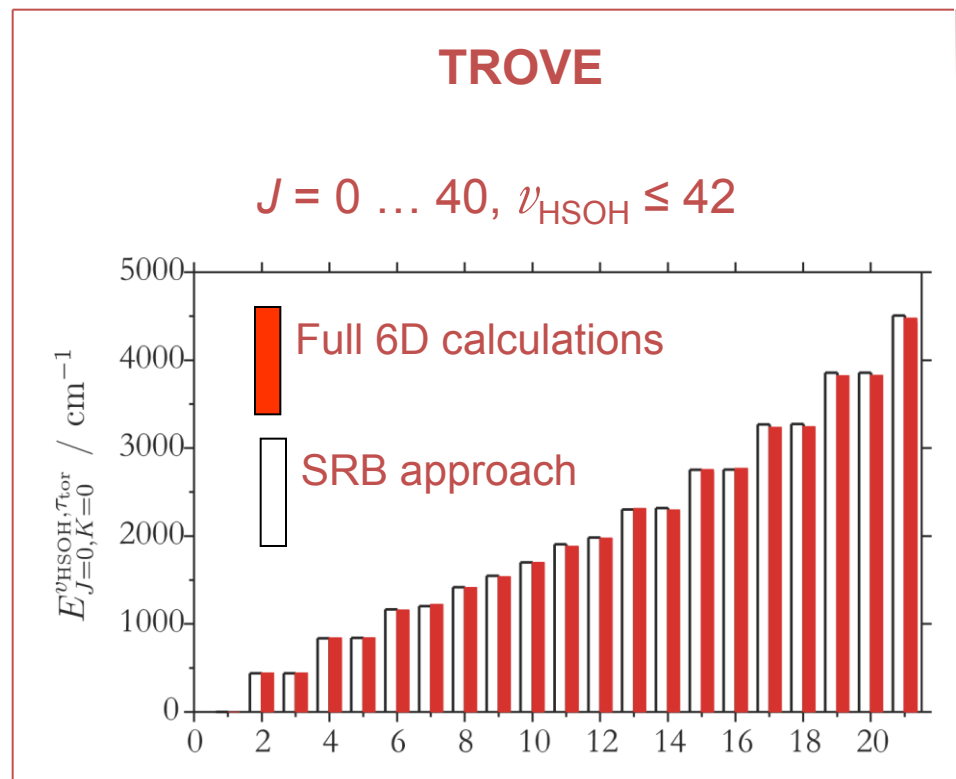
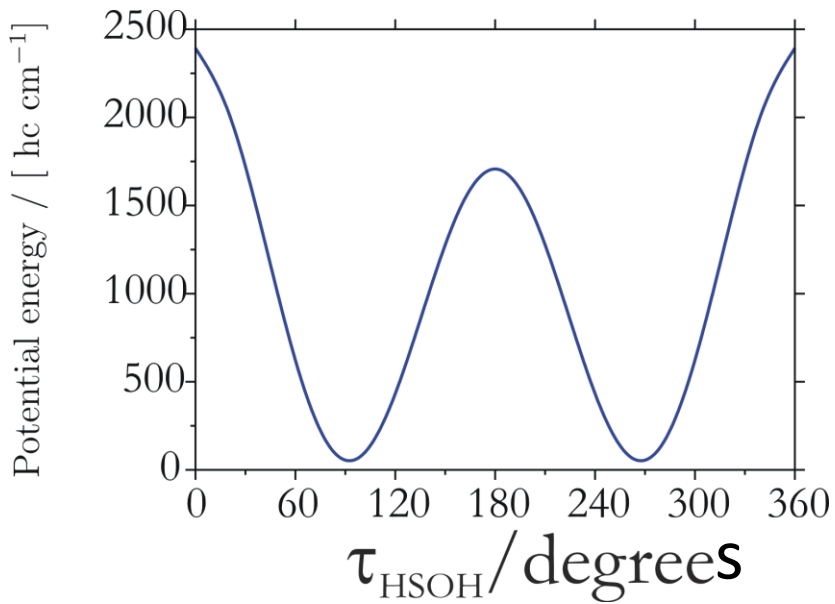
O. Baum, M. Koerber, O. Ricken, G. Winnewisser, S. N. Yurchenko, S. Schlemmer, K. M. T. Yamada, and T. F. Giesen, *J. Chem. Phys.* **129**, 224312 (2008).

Ab initio potential energy surface + TROVE calculation of torsional splittings

Ab initio potential energy surface:

- CCSD(T) method
- 105000 data points with aug-cc-pVTZ basis set, energies up to 20000 cm⁻¹ above equilibrium
- 10168 data points with aug-cc-PV(Q+d)Z basis set, energies up to 12000 cm⁻¹ above equilibrium
- Simultaneous, weighted fitting to all data points, 762 parameters varied, standard error 2.8 cm⁻¹

HSOH: *Ab initio*
 ~12000 points
CCSD(T)/aug-cc-pV(Q+d)Z



SRB approach: expansion around MEP

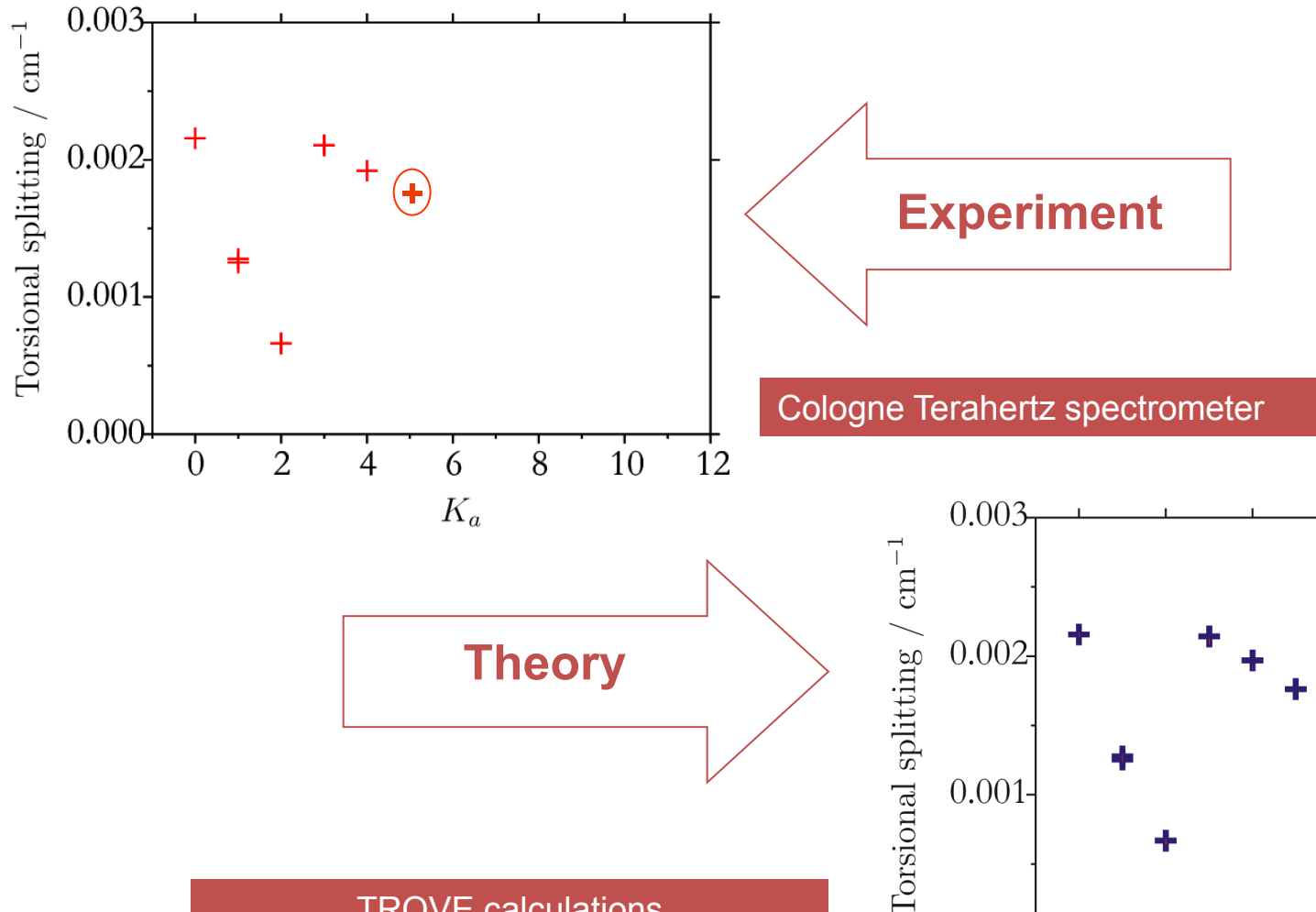
$$\Psi_{J,\Gamma,i} = |0\rangle |0\rangle |0\rangle |0\rangle |0\rangle |0\rangle \sum_{v_{\text{HSOH}}, \tau_{\text{tor}}, K, \tau_{\text{rot}}} C_{J,\Gamma,i}^{K, \tau_{\text{rot}}, v_{\text{HSOH}}, \tau_{\text{tor}}} |v_{\text{HSOH}}, \tau_{\text{tor}}\rangle |J, K, \tau_{\text{rot}}\rangle$$

HSOH rotation-torsion levels:

J	K_a	K_c	Γ	Term values (cm^{-1})			Splitting (cm^{-1})		
				obs	calc	exp-calc	calc	exp	exp-calc
4	0	4	A'	10.04696	10.05037	-0.00341			
4	0	4	A"	10.04911	10.05252	-0.00341	0.00215	0.00215	0.00000
4	1	3	A"	16.35885	16.36110	-0.00225			
4	1	3	A'	16.36011	16.36236	-0.00225	0.00126	0.00126	0.00000
4	1	4	A'	16.21151	16.21314	-0.00164			
4	1	4	A"	16.21277	16.21440	-0.00163	0.00126	0.00127	0.00000
4	2	2	A"	34.99521	34.99509	0.00011			
4	2	2	A'	34.99698	34.99694	0.00004	0.00184	0.00177	-0.00007
4	2	3	A'	34.99506	34.99495	0.00011			
4	2	3	A"	34.99683	34.99679	0.00004	0.00184	0.00177	-0.00007
4	3	1	A'	66.17016	66.17467	-0.00452			
4	3	1	A"	66.17226	66.17681	-0.00455	0.00213	0.00210	-0.00004
4	3	2	A"	66.17016	66.17467	-0.00452			
4	3	2	A'	66.17226	66.17681	-0.00455	0.00214	0.00210	-0.00004
4	4	0	A'	109.79888	109.82657	-0.02770			
4	4	0	A"	109.80079	109.82854	-0.02774	0.00196	0.00192	-0.00004
4	4	1	A"	109.79888	109.82657	-0.02770			
4	4	1	A'	109.80079	109.82854	-0.02774	0.00196	0.00192	-0.00004

Basis set: $\nu_{\text{HSOH}} \leq 42$

HSOH torsional splittings

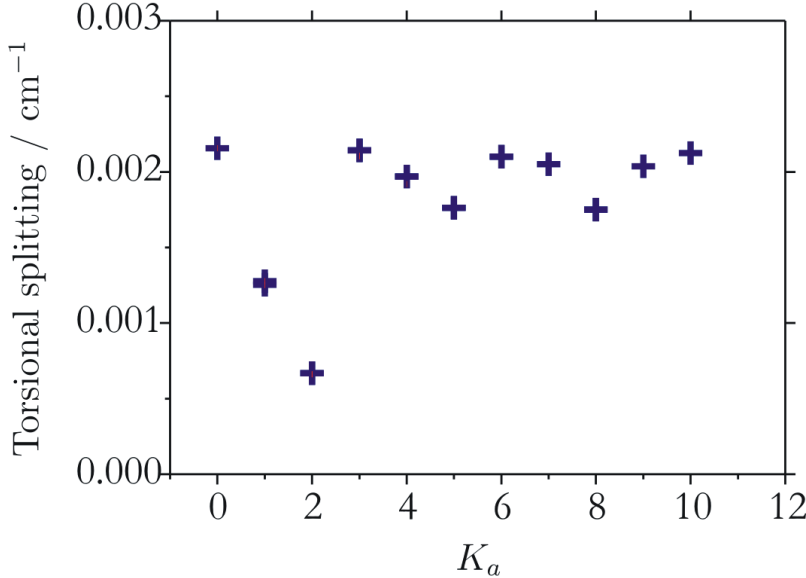


Experiment

Cologne Terahertz spectrometer

Theory

TROVE calculations



Semi-empirical alternative approach, following ideas of Hougen:

J.T. Hougen, *Can. J. Phys.* **62**, 1392 (1984).

J.T. Hougen, B.M. DeKoven, *J. Mol. Spectrosc.* **98**, 375 (1983).

Ratio of I_a moments of inertia $I_{\text{SH}}/I_{\text{total}} \approx 1/3$.

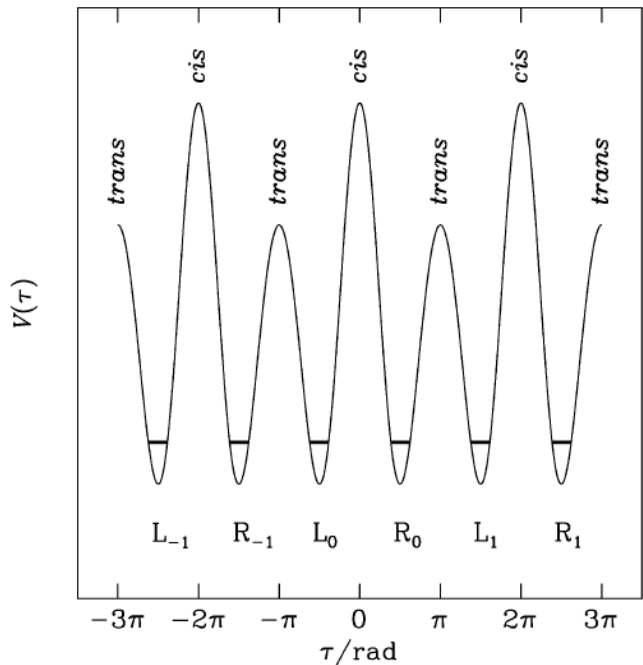
Pretend that $\tau_{\text{HSOH}} \in [-3\pi, 3\pi]$

Molecule formally has $C_{3v}(M)$ symmetry

Do quantum mechanics under this assumption.

Subject results to „reality check“: A 2π rotation of the SH moiety relative to OH moiety must leave wavefunction unchanged.

Semi-empirical alternative approach, following ideas of Hougen:



$$\tau_{HSOH} \in [-3\pi, 3\pi]$$

6 × 6 matrix:

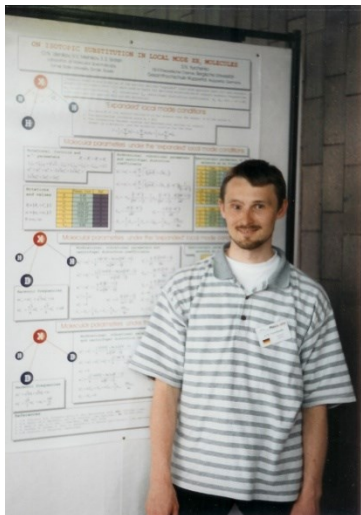
$$\begin{pmatrix} Q & W_c & 0 & 0 & 0 & W_t \\ W_c & Q & W_t & 0 & 0 & 0 \\ 0 & W_t & Q & W_c & 0 & 0 \\ 0 & 0 & W_c & Q & W_t & 0 \\ 0 & 0 & 0 & W_t & Q & W_c \\ W_t & 0 & 0 & 0 & W_c & Q \end{pmatrix}$$

HSOH splittings (2009):

The torsional splittings of HSOH in the ground state for each K .

K	Δ_{tor}	Observed ^a /MHz	Calculated ^b /MHz
0	$2 W_c + W_t $	64.5	63.9
1	$2 W_c + W_t/2 - D_{ab} $	37.8	33.3
2	$2\sqrt{(W_c - W_t/2 + 2D_{ab})^2 + 3W_t^2/4}$	52.1	50.9
3	$2 W_c + W_t - 9D_{12}^2/2(W_c + W_t) $	62.9	63.5
4	$2\sqrt{(W_c - W_t/2 - 4D_{ab})^2 + 3W_t^2/4}$	57.2	57.3
5	$2\sqrt{(W_c - W_t/2 + 5D_{ab})^2 + 3W_t^2/4}$	49.0	49.2
6	$2 W_c + W_t - 36D_{12}^2/2(W_c + W_t) $		62.1
7	$2\sqrt{(W_c - W_t/2 - 7D_{ab})^2 + 3W_t^2/4}$		61.6
8	$2\sqrt{(W_c - W_t/2 + 8D_{ab})^2 + 3W_t^2/4}$		48.6
9	$2 W_c + W_t - 81D_{12}^2/2(W_c + W_t) $		59.9
10	$2\sqrt{(W_c - W_t/2 - 10D_{ab})^2 + 3W_t^2/4}$		66.6

Thanks & Acknowledgments



The principal doer:

Sergei N. Yurchenko, Wuppertal, Ottawa,
Mülheim, Dresden, London

Other doers:

Oliver Baum, Cologne

Vladlen Melnikov, Wuppertal

Roman Ovsyannikov, Wuppertal

Andrei Yachmenev, Mülheim

Fellow ponderers:

Thomas Giesen, Cologne

Walter Thiel, Mülheim

Thanks for support from the European Commission,
the German Research Council (DFG), and the Foundation
of the German Chemical Industry (Fonds der Chemie).